J Comput Aided Mol Des (2010) 24:961–970
DOI 10.1007/s10822-010-9389-6

Prodrugs of aza nucleosides based on proton transfer reaction

Rafik Karaman

Received: 18 May 2010 / Accepted: 1 October 2010 / Published online: 13 October 2010

Abstract DFT calculation results for intramolecular proton transfer reactions in Kirby's enzyme models **1–7** reveal that the reaction rate is quite responsive to geometric disposition, especially to distance between the two reactive centers, r_{GM}, and the angle of attack, α (the hydrogen bonding angle). Hence, the study on the systems reported herein could provide a good basis for designing aza nucleoside prodrug systems that are less hydrophilic than their parental drugs and can be used, in different dosage forms, to release the parent drug in a controlled manner. For example, based on the calculated log EM, the cleavage process for prodrug **1ProD** is predicted to be about 10^{10} times faster than that for prodrug **7ProD** and about 10^4 times faster than prodrug **3ProD**: $\text{rate}_{\mathbf{1ProD}} > \text{rate}_{\mathbf{3ProD}} > \text{rate}_{\mathbf{7ProD}}$. Hence, the rate by which the prodrug releases the aza nucleoside drug can be determined according to the structural features of the linker (Kirby's enzyme model).

Keywords Aza nucleosides prodrugs · Decitabine prodrugs · DFT calculations · Proton transfer reaction · Kirby's enzyme model · Effective molarity (EM)

Introduction

The myelodysplastic syndromes (MDS, formerly known as "preleukemia") are a diverse collection of hematological conditions united by ineffective production of blood cells and varying risks of transformation to acute myelogenous leukemia (AML). Anemia requiring chronic blood transfusion is frequently present [1].

With the exception of allogeneic blood stem cell transplantation, no current treatment of patients with high-risk MDS results in a high rate of cure. However, because the median age at diagnosis of a MDS is between 60 and 75 years, and allogeneic transplantation is performed in only subset of these patients, the majority of older MDS patients currently are offered best supportive care and, despite lack of a survival benefit, low-dose chemotherapy such as low dose cytarabine.

Three agents have been approved by the U.S. Food and Drug Administration for the treatment of MDS: 5-azacitidine, decitabine and cytarabine (Scheme 1). Chemotherapy with the hypomethylating agents 5-azacytidine and decitabine has been shown to decrease blood transfusion requirements and to retard the progression of MDS to AML. All three nucleosides have a relatively short terminal elimination ($t_{1/2}$). Design and synthesis of a slow degrading prodrug can provide sustained exposure to the drug during maintenance treatment of MDS patients. This might result in better clinical outcome, more convenient dosing regimens and potentially less side effects.

For example, azacitidine is given by SC injection resulting in peak plasma concentration following administration. If a slow release prodrug can be prepared, then C_{max} related side effects may be avoided and longer duration exposure may be achieved resulting in potentially better maintenance paradigm. Another example, decitabine has to be administered by continuous IV infusion. If a controlled degrading prodrug can be provided for administration by SC injection. This could be optimum option for MDS maintenance patients on treatment [2–6].

Electronic supplementary material The online version of this article (doi:10.1007/s10822-010-9389-6) contains supplementary material, which is available to authorized users.

R. Karaman (✉)
Faculty of Pharmacy, Al-Quds University,
P. O. Box 20002, Jerusalem, Palestine
e-mail: dr_karaman@yahoo.com

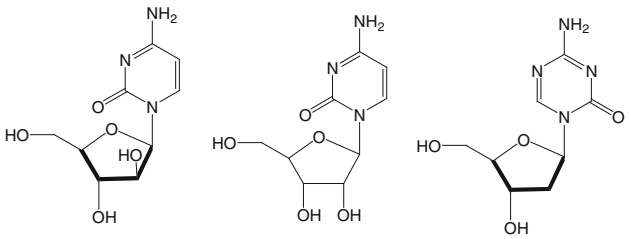

Scheme 1 Chemical structures for aza nucleoside drugs

Improvement of azacitidine, cytarabine and decitabine pharmacokinetic properties and hence their effectiveness may increase the absorption of the drug via a variety of administration routes, especially the SC injection route. This can be achieved by utilizing a carrier-linked prodrug strategy which could be done by linking the aza nucleoside drugs to a carrier moiety to furnish a drug-host system capable of penetrating the membrane tissues and librating the aza nucleoside in a controlled manner.

For achieving this goal, the aza nucleoside prodrug must possess the following properties: (1) to be readily soluble in a physiological environment (2) to have a moderate hydrophilic lipophylic balance (HLB) value (3) to provide upon chemical cleavage the active drug in a controlled manner, and (4) to furnish upon cleavage a safe and non-toxic by-products. By complying with the four requirements described above the following goals may be achieved: (1) a relatively high absorption of the pro-drug into the body tissues. (2) The capability to use the drug in different dosage forms. (3) A chemically driven sustained release system that releases the aza nucleoside drug in a controlled manner once the prodrug reaches the human blood circulation system; and (4) a drug with physical–chemical properties such that leading to a high bioavailability and efficient pharmacokinetic properties.

Recently we have been researching the driving force(s) responsible for the accelerations in rate of some intramolecular processes that were utilized as enzyme models and pro-prodrug hosts [7–23]. Using DFT and ab initio calculation methods, we have explored: 1) the acid-catalyzed lactonization of the trimethyl-lock system and other hydroxy-acids as studied by Cohen [24–29] and Menger [30–35]; (b) the intramolecular proton-transfer from oxygen to carbon in some rigid systems as researched by Menger [30–35]; (c) the S_N2-based ring-closing reactions as investigated by Brown, Bruice and Mandolini [36–39] and (d) the proton transfer between two oxygen atoms in some of Kirby's acetals [40–49]. Our study on the above systems revealed the following: accelerations in rate for intramolecular reactions are a result of both entropy and enthalpy effects. In the cases by which enthalpic effects were predominant proximity or/and steric effects were the driving force for rate enhancements. In addition, we have found that efficient proton transfer in Kirby's acetal systems was achieved when a strong hydrogen bonding was developed in the products and the corresponding transition states leading to them.

It is worth noting that our previous studies stress the need to unravel the reaction mechanism and to identify the driving force affecting the reaction rate in order to design an efficient chemical device (pro-drug). The designed prodrugs should have the potential to undergo cleavage reactions in physiological environments in rates that are completely dependent on the structural features of the host (inactive linker) [10–23].

Continuing our study in this area, we sought to investigate the driving forces responsible for accelerations in rate of proton transfer reactions in some of Kirby's enzyme models [40–49]. It is expected that such molecules have the potential of being good carriers to the anti-preleukemia aza neoclosides. Our proposed aza nucleoside prodrug systems based on proton transfer reaction is depicted in Scheme 2.

Based on our reported DFT calculations herein on a proton transfer reaction in some of Kirby's enzyme models, three prodrugs of aza nucleoside are proposed. As shown in Scheme 2, the aza nucleoside prodrugs, **1ProD**, **3ProD** and **7ProD** have N, N-dimethylanilinium group (hydrophilic moiety) and a lipophilic moiety (the rest of the prodrug), where the combination of both moieties secures a moderate HLB. Furthermore, in a physiologic environment of pH 5.5, SC, prodrugs **1ProD**, **3ProD** and **7ProD** may have a better bioavailability than the parent drugs due to improved absorption. In addition, those prodrugs may be used in different dosage forms (i.e. enteric coated tablets) because of their potential solubility in organic and aqueous media due to the ability of the anilinium group to be converted to the corresponding aniline group in a physiological pH of 6.5.

It should be emphasized that at pH 5.5–6.5 (SC and intestine physiologic environments) the anilinium form of those pro-drugs will equilibrate with the free aniline form. Subsequently, the former will undergo proton transfer reaction (rate limiting step) to yield the anti-preleukemia aza neocloside drug and the inactive carrier as a by-product (Scheme 2).

Calculations methods

The DFT calculations were carried out using the quantum chemical package Gaussian-98 [50]. The starting

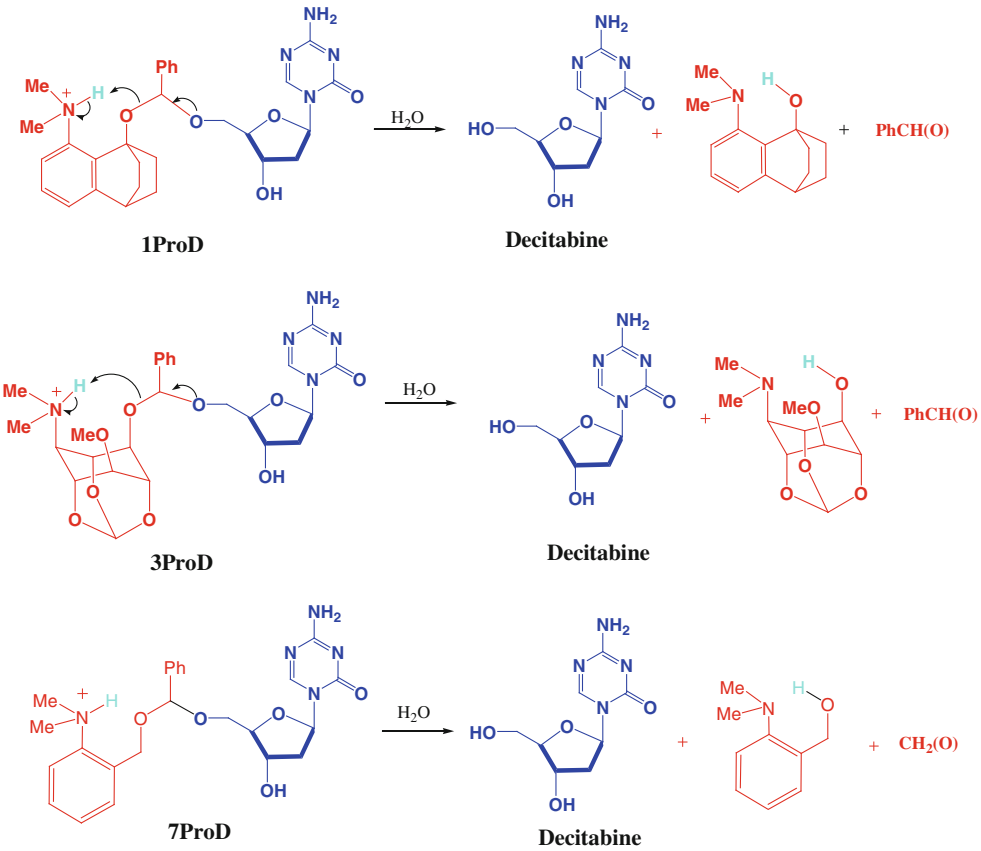

Scheme 2 Proposed mechanism for the chemical cleavage of **1ProD**, **3ProD** and **7ProD** to their corresponding parental drugs

geometries of all the molecules presented in this study were obtained using the Argus Lab program [51] and were initially optimized at the AM1 and HF/6-31G levels of theory [52]. The calculations were carried out based on the restricted Hartree–Fock (RHF) method with full optimization of all geometrical variables. An energy minimum (a stable compound or a reactive intermediate) has no negative vibrational force constant. A transition state is a saddle point which has only one negative vibrational force constant [53]. The "reaction coordinate method" [54] was used to calculate the activation energy in systems **1–7**. In this method, one bond length is constrained for the appropriate degree of freedom while all other variables are freely optimized. The activation energy values for the proton transfer reactions were calculated from the difference in energies of the global minimum structure and the derived transition state (TS). Verification of the desired reactants and products was accomplished using the "intrinsic coordinate method" [54]. The transition state structures were verified by their only one negative frequency. Full optimization of the transition states was accomplished after removing any constrains imposed while executing the energy profile. The activation energies obtained from the DFT calculations for **1–7** were calculated with the inclusion of one and two molecules of water.

Results and discussion

To achieve an efficient pharmacological activity of the three aza nucleosides (relatively hydrophilic systems) shown in Scheme 1, the prodrug approach of linking the aza nucleoside moiety (parental drug) to a relatively hydrophobic inactive host, which upon reaching the physiologic environment, releases the parental drug seems to be a successful strategy. The proposed aza nucleosides prodrugs shown in Scheme 2 are less hydrophilic than the parental drug. Thus enabling the prodrug to penetrate the membrane tissues in much better extent than the parental drug and consequently to prolong the pharmacological activity and to improve the anti myelogenous leukemia therapeutic strategy. Kirby's novel study on some enzyme models has inspired us to utilize these systems as potential linkers to the aza nucleoside drugs depicted in Scheme 1. It should be emphasized that our proposal is to exploit prodrugs **1ProD**, **3ProD** and **7ProD** for S.C. use. The physiologic environment of the skin has a pH of 5.5. At physiologic environment of pH 5.5 prodrugs **1ProD**, **3ProD** and **7ProD** is predicted to exist in the unionized (free base) and ionized (ammonium) forms where the equilibrium constant for the exchange between both forms is dependent on the pK_a of the given prodrug. The experimental determined pK_a for N, N-dimethylanilin is 5.15

[55] hence it is expected that the pK_a values for prodrugs **1ProD**, **3ProD** and **7ProD** will be in the same range. Since the pH for the skin lies in the range around 5.5, the calculated ionized (ammonium)/unionized (free base) ratio will be 69/31 (see Eq. 1) [56].

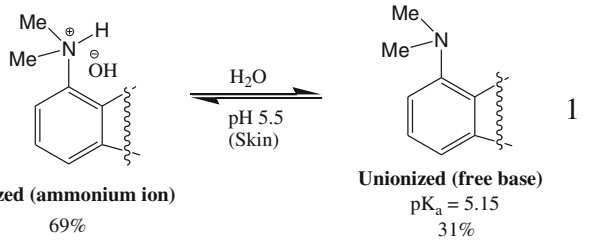

Ionized (ammonium ion)
69%

Unionized (free base)
$pK_a = 5.15$
31%

1

1

It is quite safe to assume that the unionized forms for prodrugs **1ProD**, **3ProD** and **7ProD** (see Eq. 1) will be more lipophilic than the parental drugs due the presence of a relatively bulky group (Kirby's enzyme model linker). Therefore, the absorption of those prodrugs through the skin membranes and the efficiency for delivering the parental drug are expected to be increased. If the prodrugs **1ProD**, **3ProD** and **7ProD** are intended to be delivered by per os dosage form, for example as an enteric coated tablets, the absorption and consequently the efficiency of those prodrugs will be relatively reduced compared to the SC route. This is because the calculated percentage of the unionized form, in the case where the absorption is taking place in the small intestine (pH = 6.5), is predicted in the range of 5–31% [56].

The selection of Kirby's enzyme models to be utilized as carriers to aza nucleosides is based on the fact that those carriers undergo proton transfer reaction to yield an aldehyde, an alcohol and a hydroxy amine (Scheme 3). The rate-limiting step in these processes (processes **1–7**, Scheme 3) is a transfer of a proton from the anilinium group into the neighboring ether oxygen. Furthermore, the proton transfer rate is strongly dependent on the strength of the hydrogen bonding in the products and in the transition states leading to them [40–49]. Therefore, it will be safe to assume that the reaction rate will be greatly affected by the structural features of the enzyme model system as evident from the different experimental rate values determined for processes **1–3** [40–49].

Replacing the methoxy group in **1–7** (Scheme 3) with aza nucleoside drug, as shown for **1ProD**, **3ProD** and **7ProD** in Scheme 2, is not expected to have any significant effect on the relative rates of these processes. Therefore, computational calculations of the kinetic and thermodynamic properties for these models will shed some light on the rates for the chemical cleavage of pro-drugs **1ProD**, **3ProD** and **7ProD** to the corresponding aza nucleoside drugs.

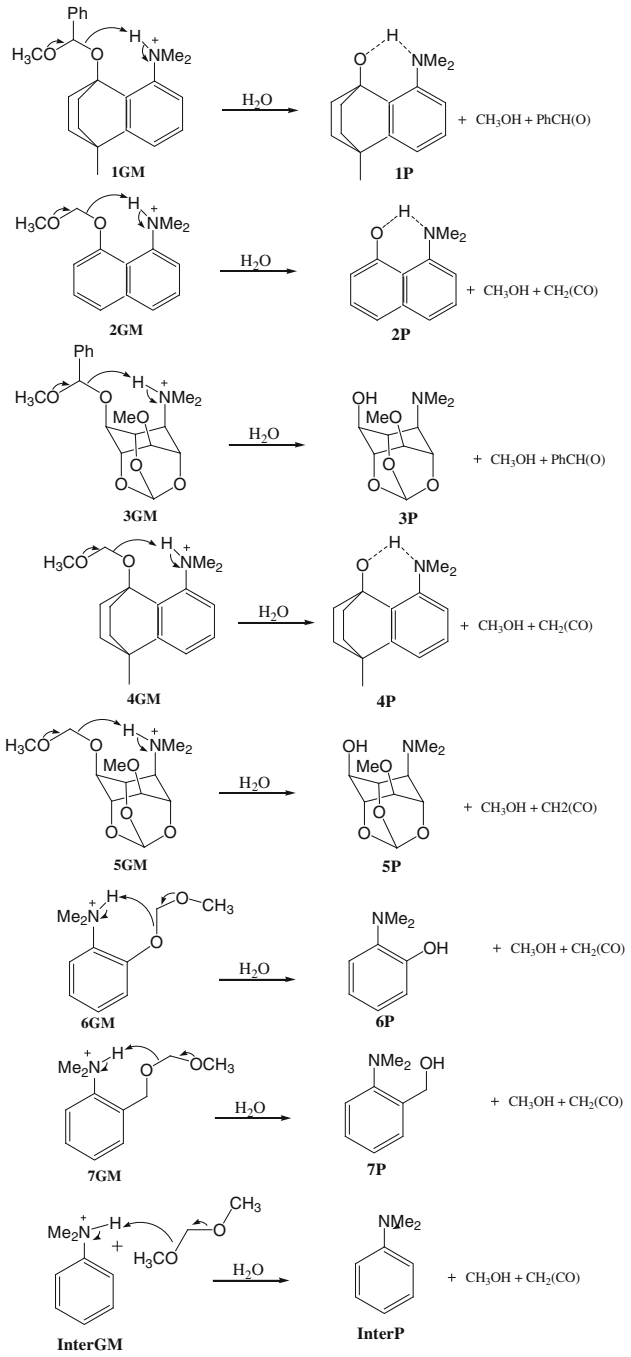

Scheme 3 Proposed mechanism for Kirby's enzyme model **1–7** and their corresponding intermolecular process

Conformational analysis for the entities involved in the proton transfer reactions of Kirby's enzyme models 1–7

Starting geometries (GM)

Since the proton transfer reactions for Kirby's enzyme models **1–7** were carried out in aqueous medium, we have

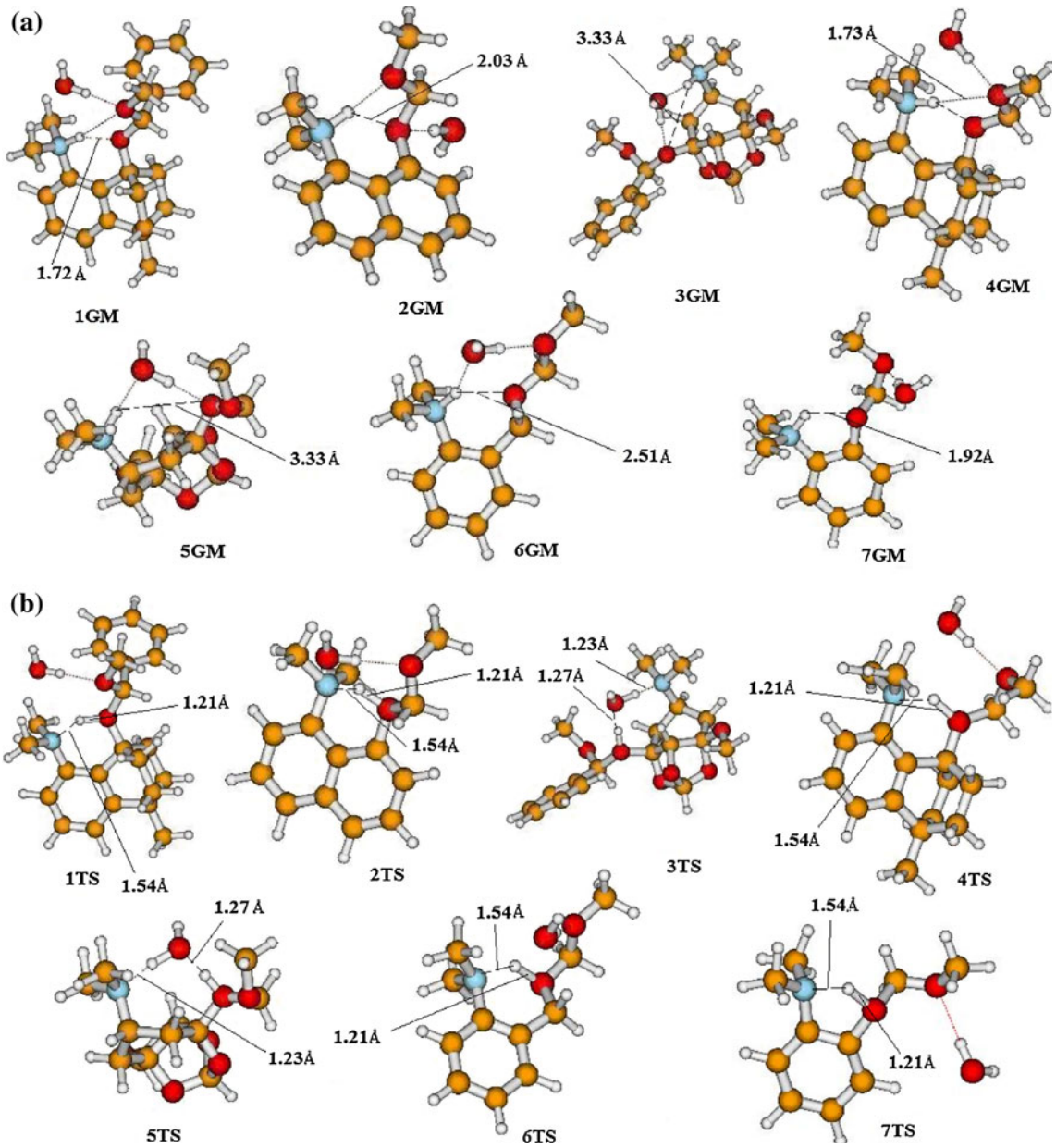

Fig. 1 **a** DFT optimized structures for **1GM–7GM**. **b** DFT optimized structures for **1TS–7TS**

calculated the geometries of the entities involved in these processes in the presence of one and two molecules of water. The DFT calculated properties for the starting geometries of **1–7** (**1GM–7GM**) are shown in Fig. 1a and Table 1. Inspection of the calculated geometries of **1GM–7GM** indicates that all of them except **3GM** and **5GM** exhibit conformation by which the anilinium group is engaged intramolecularly in a hydrogen bonding net with the neighboring alkoxy oxygen. This engagement results in the formation of six-membered ring for **1GM**, **2GM**, **4GM** and **6GM** and five-membered ring for **7GM** (see Fig. 1a). The DFT calculated hydrogen bonding length for **1GM–3GM** and **5GM–6GM** was found in the range of 1.72–2.51 Å and that for the attack angle α (the hydrogen bond angle, $N_1H_2O_3$) in the range of 107°–146°. Furthermore, the hydrogen bonding strength, r_{GM} (H_2-O_3), varies according to the structural features of the starting geometry (for the definition of r_{GM} and α see Scheme 4). On the other hand, no intramolecular hydrogen bond was found in the global minimum structures of **3** and **5** (**3GM** and **5 GM**). The interatomic distance, r_{GM} (H_2-O_3), between the ammonium proton and the ether oxygen in **3GM** and **5 GM** is 3.33 Å (Fig. 1a and Table 1). The optimized global minimum structures for **3** and **5** were found to be intermolecularly engaged with a water molecule where the latter hydrogen bonds with both the ammonium and the ether groups.

Table 1 DFT (B3LYP/6-31G (d,p)) calculated kinetic and thermodynamic properties for the proton transfer in **1–7**

System	Medium	H_2-O_3 r_{GM}	$N_1H_2O_3$ α	β	$\Delta H^{\ddagger}$	$T\Delta S^{\ddagger}$	$\Delta G^{\ddagger}$	Log EM (calc.)
1	$1H_2O$	1.72	146	140	23.62	0.07	23.55	1.67
	$2H_2O$	1.72	146	140	23.78	0.99	22.79	
2	$1H_2O$	2.04	125	125	24.73	−3.34	28.07	−1.65
	$2H_2O$	2.04	125	125	24.73	−3.34	28.07	
3	$1H_2O$	3.33	123	–	25.41	−4.15	29.56	−2.75
	$2H_2O$	3.33	123	–	39.54	−4.29	43.83	
4	$1H_2O$	1.73	144	145	22.54	0.90	21.64	3.07
	$2H_2O$	1.73	144	145	21.24	0.88	20.39	
5	$1H_2O$	3.33	124	–	23.59	−4.15	27.74	−1.41
	$2H_2O$	3.33	124	–	25.67	−1.21	26.88	
6	$1H_2O$	1.92	122	122	29.33	0.61	28.72	−2.13
	$2H_2O$	1.92	122	122	23.00	3.90	19.10	
7	$1H_2O$	2.51	107	133	34.71	−2.00	36.71	−8.01
	$2H_2O$	2.51	107	133	29.73	−0.01	29.74	

$\Delta H^{\ddagger}$ is the activation enthalpic energy (kcal/mol). $T\Delta S^{\ddagger}$ is the activation entropic energy in kcal/mol

$\Delta G^{\ddagger}$ is the activation free energy (kcal/mol). α is the hydrogen bonding angle in the ground state structure (see Scheme 4). β is the hydrogen bonding angle in the ground state structure (see Scheme 4) $EM = e^{-\left(\Delta G^{\ddagger}_{inter} - \Delta G^{\ddagger}_{intra}\right)/RT}$

Transition state geometries (TS)

The DFT calculated properties for the transition state geometries of **1–7** (**1TS–7TS**) are illustrated in Fig. 1b and Table 1. Examination of the calculated structures for **1TS–7TS** reveals that all the geometries involve a strong hydrogen bonding between the ammonium proton and the ether oxygen except for **3TS** and **5TS** where the optimized geometries exist in a conformation by which the ammonium and the ether groups engage in a hydrogen bonding with a molecule of water.

Calculating the proton transfer rate (activation energy, $\Delta G^{\ddagger}$) in Kirby's enzyme models 1–7

Using the quantum chemical package Gaussian-98 [50] we have computed the DFT B3LYP/6-31G (d,p) kinetic and thermodynamic parameters for the intramolecular proton transfer in processes **1–7** (Scheme 3).

The B3LYP/6-31G (d,p) activation energy values were calculated with the inclusion of one and two molecules of water.

Using the DFT calculated enthalpic and entropic energies for the global minimum structures **1GM–7GM** (H_{GM}) and the derived transition states **1TS–7TS** (H_{TS}) (Table 2) we have calculated the enthalpic ($\Delta H^{\ddagger}$), the entropic ($T\Delta S^{\ddagger}$), and the free activation energies ($\Delta G^{\ddagger}$) for the corresponding proton transfer reactions. The calculated values are summarized in Table 1.

The role of the distance r_{GM} and the angle α on the reaction rate for the proton transfer in processes 1–7

As previously mentioned, the calculation results for **1GM–6GM** revealed the existence of intramolecular hydrogen bonding between the ammonium group N_1–H_2 and the ether oxygen O_3 where the distance between the two reacting centers r_{GM} (H_2-O_3) is determined on the structural features of the conformation in which the global minimum structure resides. Short r_{GM} distances were obtained when the hydrogen bonding angle (α) value (see Scheme 4) in the reactant conformation was high and close to 180°, whereas small values of α resulted in longer r_{GM} distances (Fig. 1a and Table 1). Furthermore, when r_{GM} and α were examined for linear relationship strong correlation with a high correlation coefficient was found between the two parameters (Fig. 2a).

In addition, Table 1 reveals that the free activation energy ($\Delta G^{\ddagger}$) needed to execute a proton transfer in systems **1–7** is largely affected by both the distance r_{GM} (H_2-O_3), and the hydrogen bonding angle α ($N_1H_2O_3$) (see Scheme 4). Systems with low r_{GM} and high α values in their global minimum structures, such as **1** and **4**, exhibit much higher rates (lower $\Delta G^{\ddagger}$) than those having high r_{GM} and low α values, such as **3** and **7**. Linear correlation of the calculated DFT free activation ($\Delta G^{\ddagger}$) and enthalpic activation energies ($\Delta H^{\ddagger}$) with $r^2_{GM} \times \sin(180\text{-}\alpha)$ values gave good correlations with a relatively high correlation coefficients, $R = 0.98$ and 0.92, respectively (Fig. 2b, c).

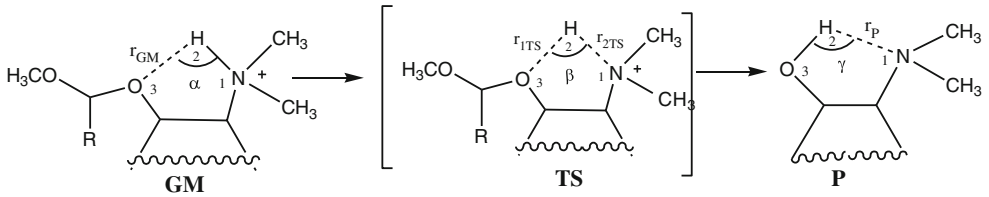

Scheme 4 Schematic representation of the proton transfer in Kirby's enzyme models **1–7**. GM, TS and P are global minimum, transition state and product structures, respectively. α, β and γ are the angle N_1–H_2–O_3 in the GM, TS and P, respectively. r_{GM}, r_{TS} and r_P are the distances between the two reacting centers in the GM, TS and P, respectively. R is H or phenyl

Table 2 DFT (B3LYP/6-31G (d,p)) calculated properties for the proton transfer reactions of **1–7**

Compound	DFT Enthalpy, H ($1H_2O$) (In Hartree)	DFT ($1H_2O$) Entropy, S (Cal/Mol-Kelvin)	DFT ($1H_2O$) Frequency (Cm^{-1})	DFT Enthalpy, H ($2H_2O$) (In Hartree)	DFT ($2H_2O$) Entropy, S, (Cal/Mol − Kelvin)	DFT ($2H_2O$) Frequency (Cm^{-1})
1GM	−1175.983529	177.14	–	−1252.402543	186.91	–
1TS	−1175.945886	177.33	1211.54i	−1252.586002	190.26	1208.59i
2GM	−825.744864	144.14	–	−902.157231	147.89	–
2TS	−825.705451	132.94	1183.58i	−902.117912	136.67	1177.31i
3GM	−1283.868047	170.25	–	−1360.291217	177.52	–
3TS	−1283.827552	156.33	540.07i	−1360.228202	163.14	574.42i
4GM	−944.9179278	148.81	–	−1021.334786	157.93	–
4TS	−944.8827078	151.82	1204.52i	−1021.300936	160.78	1219.01i
5GM	−1052.8077145	146.32	–	−1129.232067	156.03	–
5TS	−1052.7701241	142.31	104.33i	−1129.191158	151.97	107.12i
6GM	−672.0864671	128.64	–	−748.496382	133.99	–
6TS	−672.0397241	130.69	1216.61i	−748.459726	147.08	1229.44i
7GM	−711.435482	134.51	–	−787.858192	146.35	–
7TS	−711.380168	127.78	1125.45i	−787.810809	146.31	1147.77i

GM and TS are global minimum and transition state structures, respectively

*The effect of the R group (Scheme 4) on the reaction rate of the proton transfers in **1–7***

In order to investigate the importance of the R group (Scheme 4) on the efficiency of the proton transfer the activation energies for processes **1** and **3** (R=phenyl), on one hand, and **4** and **5** (R=H), on the other hand, were compared. Examination of Table 1 reveals no significant change in the r_{GM} distance and the attack angle α values upon changing the R group from a phenyl to a hydrogen group. On the other hand, the calculation results indicate that systems having R=H such as **4** and **5** were found to be more efficient than their corresponding phenyl derivatives as it evident from their DFT calculated free activation energies ($\Delta G^{\ddagger}$). For example, the $\Delta G^{\ddagger}$ for process **1** is 23.55 kcal/mol whereas for **4** is 21.64 kcal/mol (Table 1). This discrepancy in rates might be attributed to the electron withdrawing effect of the phenyl group in the case of processes **1** and **4**.

*Calculating the effective molarities (EM) in Kirby's enzyme models **1–7***

The effective molarity (EM) is defined as the rate ratio (k_{intra}/k_{inter}) for intramolecular and corresponding intermolecular processes driven by identical mechanisms. The effective molarity is considered an excellent tool for the evaluation of the efficiency of a certain intramolecular process [57]. Since the EM values for some processes shown in Scheme 3 are not available we sought to introduce our computational rational for calculating these values based on the DFT calculated activation energies ($\Delta G^{\ddagger}$) for **1–7** and the corresponding intermolecular process (Scheme 3), where process **Inter** (Scheme 3) was chosen to represent the corresponding intermolecular process for **1–7**.

Equation 6 derived from Eqs. 2–5 describes the EM term as a function of the difference in the activation energies of the intra- and the corresponding inter-molecular processes. The calculated EM values for processes **1–7** listed in Table 1 were calculated using Eq. 6.

$$EM = k_{intra}/k_{inter} \tag{2}$$

$$\Delta G^{\ddagger}_{inter} = -RT \ln k_{inter} \tag{3}$$

$$\Delta G^{\ddagger}_{intra} = -RT \ln k_{intra} \tag{4}$$

$$\Delta G^{\ddagger}_{intra} - \Delta G^{\ddagger}_{inter} = -RT \ln k_{intra}/k_{inter} \tag{5}$$

$$EM = e^{-\left(\Delta G^{\ddagger}_{inter} - \Delta G^{\ddagger}_{inter}\right)/RT} \tag{6}$$

where T is 298° K and R is the gas constant.

The DFT calculated values for **1–7** were examined for linear correlation with the enthalpic ($\Delta H^{\ddagger}$) and free activation ($\Delta G^{\ddagger}$) energies. The correlation results along with the correlation coefficients are illustrated in Fig. 2d. Inspection of the EM values listed in Table 1 and Fig. 2d revealed that **1** and **4** are the most efficient processes among **1–7** (log EM = 2–3) and the least efficient is process **7** with log EM < −8. Although the EM values for **1–7** were not experimentally determined, Kirby and coworkers estimated the experimental log EM value for process **1** in the order of 3 [40–49]. The calculated DFT EM values for **1** and **4** are 1.67 and 3.07, respectively. Theses values are

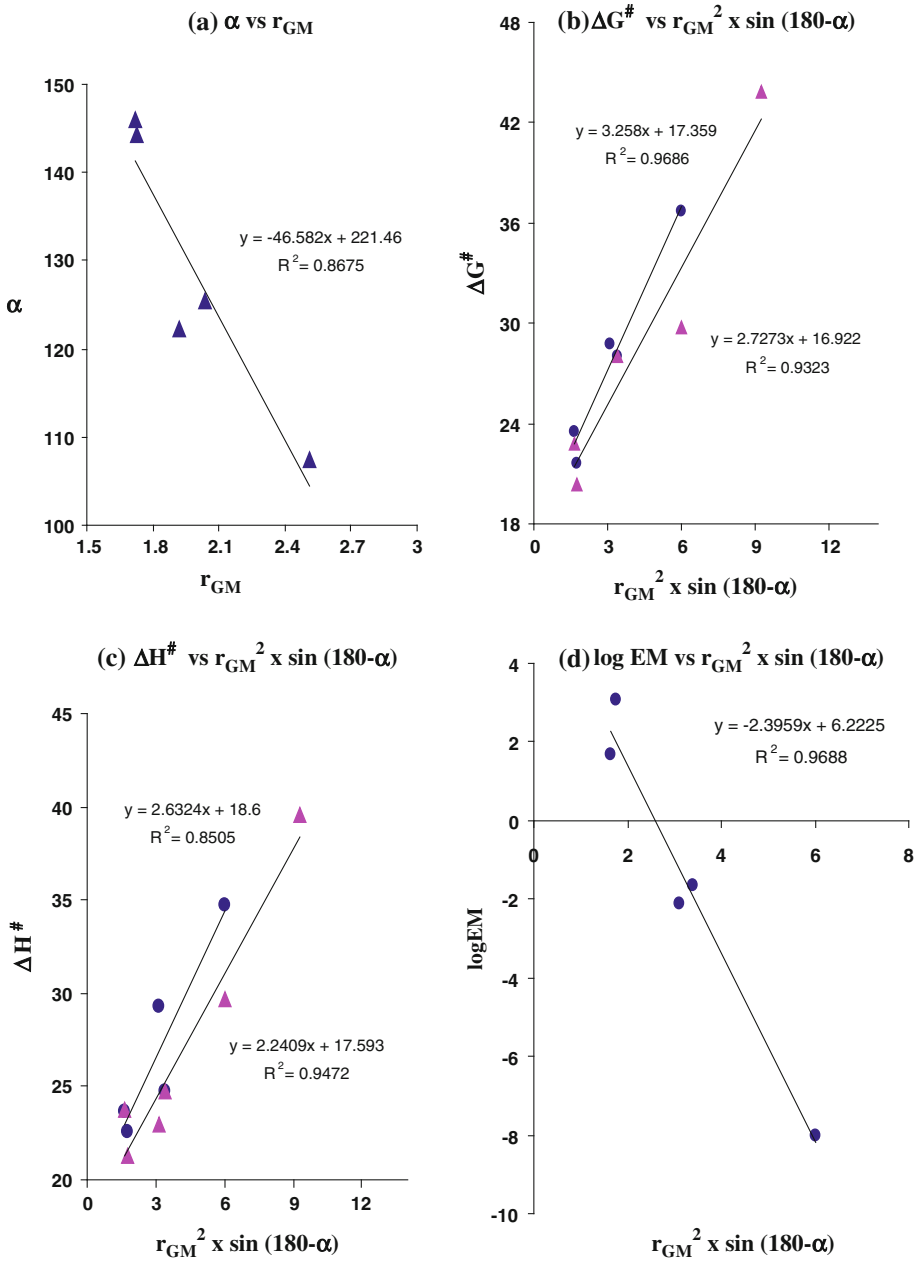

Fig. 2 **a** Plot of the DFT calculated α versus r_{GM} in **1–7**, where α is the attack angle in the GM structure. **b** Plot of the DFT calculated $\Delta G^{\ddagger}$ versus $r_{GM}^2 \times \sin(180\text{-}\alpha)$ in **1–7**, where r_{GM} is the distance between the two reactive centers. The *blue* and the *pink points* are for the DFT calculated GM in the presence of $1H_2O$ and $2H_2O$, respectively. **c** Plot of the DFT calculated $\Delta H^{\ddagger}$ versus $r_{GM}^2 \times \sin(180\text{-}\alpha)$ in **1–7**. The *blue* and the *pink points* are for the DFT calculated GM in the presence of $1H_2O$ and $2H_2O$, respectively. **d** Plot of the DFT calculated log EM versus $r_{GM}^2 \times \sin(180\text{-}\alpha)$ in **1–7**, where EM is the calculated effective molarity (see text)

in agreement with the corresponding experimental estimated values.

Conclusions and future directions

The DFT calculation results indicate that the proton transfer rate in processes **1–7** is quite responsive to geometric disposition, especially to distance between the two reactive centers, r_{GM}, and the angle of attack, α (the hydrogen bonding angle). The vital requirement for a system for achieving a high intramolecular proton transfer rate is a short distance between the two reactive centers (r_{GM}) in the ground states (GM) which subsequently results in strong intramolecular hydrogen bonding in the products and the transition states leading to them.

In summary, we conclude that the computational study on systems **1–7** reported herein could provide a stepping stone for the design of prodrug systems that can be pharmaceutically used as devices for an efficient slow release of the aza nucleosides. For example, based on the calculated log EM, the cleavage process for pro-drug **1ProD** may be predicted to be about 10^{10} times faster than that for pro-drug **7ProD** and about 10^4 times faster than prodrug **3ProD**: $\text{rate}_{\mathbf{1ProD}} > \text{rate}_{\mathbf{3ProD}} > \text{rate}_{\mathbf{7ProD}}$ (Scheme 2). Hence, the

rate by which the prodrug releases the aza nucleoside drug can be determined according to the structural features of the linker (Kirby's enzyme model).

Our future directions include the synthesis of prodrug **1ProD**, **3ProD** and **7ProD** according to known procedures followed by in vitro kinetic studies at different pH values. The kinetic data results will provide the data basis for the pharmacokinetic studies, in vivo.

Based on the in vitro results, one or more of the prodrug systems will be tested in vivo in addition to aza nucleoside drug as a control. The prodrug will be administered to animals by IV, IM, SC injections and per os, blood and urine samples will be collected at different times. The concentration of the aza nucleoside will be determined using a reliable bioanalytical method. Further, pharmacokinetic parameter values will be calculated including oral bioavailability, terminal elimination half-life and other pharmacokinetic parameters as deemed necessary.

Acknowledgments The Karaman Co. and the German-Palestinian-Israeli fund agency are thanked for support of our computational facilities. Special thanks are given to Angi Karaman, Donia Karaman, Rowan Karaman and Nardene Karaman for technical assistance.

References

1. The Leukemia & Lymphoma Society (2001) Myelodysplastic syndrome. White Plains, NY
2. Wijermans P, Lübbert M, Verhoef G et al (2000) Low-dose 5-aza-2'-deoxycytidine, a DNA hypomethylating agent, for the treatment of high-risk myelodysplastic syndrome: a multicenter phase II study in elderly patients. J Clin Oncol 18:956–962
3. Silverman LR, Demakos EP, Peterson BL et al (2002) Randomized controlled trial of azacitidine in patients with the myelodysplastic syndrome: a study of the cancer and leukemia group B. J Clin Oncol 20:2429–2440
4. Silverman LR, McKenzie DR, Peterson BL et al () Further analysis of trials with azacitidine in patients with myelodysplastic syndrome: studies 8421, 8921, and 9221 by the Cancer and Leukemia Group B. J Clin Oncol 2006(24):3895–3903
5. Kantarjian H, Issa JP, Rosenfeld CS et al (2006) Decitabine improves patient outcomes in myelodysplastic syndromes: results of a phase III randomized study. Cancer 106:1794–1803
6. Blum W, Klisovic RB, Hackanson B et al (2007) Phase I study of decitabine alone or in combination with valproic acid in acute myeloid leukemia. J Clin Oncol 25:3884–3891
7. Testa B, Mayer J (2003) Hydrolysis in drug and prodrug metabolism—chemistry, biochemistry and enzymology. Wiley, Zurich
8. Testa B, Mayer JM (2001) Concepts in prodrug design to overcome pharmacokinetic problems. In: Testa B, van de Waterbeemd H, Folkers G, Guy R (eds) Pharmacokinetic optimization in drug research: biological, physiochemical and computational strategies. Wiley, Zurich, pp 85–95
9. Wang W, Jiang J, Ballard CE, Wang B (1999) Prodrug approaches in the improved delivery of peptide drugs. Curr Pharm Design 5:265–287
10. Karaman R (2008) Analysis of Menger's spatiotemporal hypothesis. Tet Lett 49:5998–6002
11. Karaman R (2009) Reevaluation of Bruice's proximity orientation. Tet Lett 50:452–456
12. Karaman R (2009) A new mathematical equation relating activation energy to bond angle and distance: a key for understanding the role of acceleration in the lactonization of the trimethyl lock system. Bioorg Chem 37(1):11–25
13. Karaman R (2009) Accelerations in the lactonization of trimethyl lock systems is due to proximity orientation and not to strain effects. Res Lett Org Chem. doi: 10.1155/2009/240253
14. Karaman R (2009) The effective molarity (EM) puzzle in proton transfer reactions. Bioorg Chem 37:106–110
15. Karaman R (2009) Cleavage of Menger's aliphatic amide: a model for peptidase enzyme solely explained by proximity orientation in intramolecular proton transfer. J Mol Struct (Theochem) 910:27–33
16. Karaman R (2009) The gem-disubstituent effect-computational study that exposes the relevance of existing theoretical models. Tet Lett 50:6083–6087
17. Karaman R (2010) Affects of substitution on the effective molarity (EM) for five membered ring-closure reactions- a computational approach. J Mol Struct (Theochem) 939:69–74
18. Karaman R (2009) Analyzing Kirby's amine olefin—a model for amino-acid ammonia lyases. Tet Lett 50:7304–7309
19. Karaman R (2010) The effective molarity (EM) puzzle in intramolecular ring-closing reactions. J Mol Struct (Theochem) 940: 70–75
20. Karaman R (2010) The efficiency of proton transfer in Kirby's enzyme model, a computational approach. Tet Lett 51:2130–2135
21. Karaman R (2010) A general equation correlating intramolecular rates with "attack" parameters distance and angle. Tet Lett 51: 5185–5190
22. Karaman R (2010) The effective molarity (EM)—a computational approach. Bioorg Chem 38:165–172
23. Karaman R (2010) Proximity vs. strain in ring-closing reactions of bifunctional chain molecules—a computational approach. J Mol Phys 108:1723–1730
24. Milstien S, Cohen LA (1970) Concurrent general-acid and general-base catalysis of esterification. J Am Chem Soc 92: 4377–4382
25. Milstien S, Cohen LA (1970) Rate acceleration by stereo population control: models for enzyme action. Proc Natl Acad Sci U S A 67:1143–1147
26. Milstien S, Cohen LA (1972) Stereopopulation control I. Rate enhancement in the lactonizations of o-hydroxyhydrocinnamic acids. J Am Chem Soc 94:9158–9165
27. Winans RE, Wilcox CF Jr (1976) Comparison of stereopopulation control with conventional steric effects in lactonization of hydrocoumarinic acids. J Am Chem Soc 98:4281–4285
28. Dorigo AE, Houk KN (1987) The origin of proximity effects on reactivity: a modified MM2 model for the rates of acid-catalyzed lactonizations of hydroxy acids. J Am Chem Soc 109:3698–3708
29. Houk KN, Tucker JA, Dorigo AE (1990) Quantitative modeling of proximity effects on organic reactivity. Acc Chem Res 23: 107–113
30. Menger FM (1985) On the source of intramolecular and enzymatic reactivity. Acc Chem Res 18:128–134
31. Menger FM, Chow JF, Kaiserman H, Vasquez PC (1983) Directionality of proton transfer in solution: three systems of known angularity. J Am Chem Soc 105:4996–5002
32. Menger FM (1983) Directionality of organic reactions in solution. Tetrahedron 39:1013–1040
33. Menger FM, Grossman J, Liotta DC (1983) Transition-state pliability in nitrogen-to-nitrogen proton transfer. J Org Chem 48: 905–907
34. Menger FM, Galloway AL, Musaev DG (2003) Relationship between rate and distance. Chem Comm 2370–2371

35. Menger FM (2005) An alternative view of enzyme catalysis. Pure Appl Chem 77:1873–1886
36. Bruice TC, Pandit UK (1960) The effect of geminal substitution ring size and rotamer distribution on the intramolecular nucleophilic catalysis of the hydrolysis of monophenyl esters of dibasic acids and the solvolysis of the intermediate anhydrides. J Am Chem Soc 82:5858–5865
37. Bruice TC, Pandit UK (1960) Intramolecular models depicting the kinetic importance of "Fit" in enzymatic catalysis. Proc Natl Acad Sci U S A 46:402–404
38. Brown RF, Van Gulick NM (1956) The geminal alkyl effect on the rates of ring closure of bromobutylamines. J Org Chem 21:1046–1049
39. Galli C, Mandolini L (2000) The role of ring strain on the ease of ring closure of bifunctional chain molecules. Eur J Org Chem 3117–3125, and references therein
40. Kirby AJ (1997) Efficiency of proton transfer catalysis in models and enzymes. Acc Chem Res 30:290–296
41. Brown CJ, Kirby AJ (1997) Efficiency of proton transfer catalysis: intramolecular general acid catalysis of the hydrolysis of dialkyl acetals of benzaldehyde. J Chem Soc Perkin Trans 2:1081–1093
42. Craze GA, Kirby AJ (1974) The role of carboxy-group in intramolecular catalysis of acetal hydrolysis: the hydrolysis of substituted 2-methoxymethoxybenzoic acids. J Chem Soc Perkin Trans 2:61–66
43. Barber SE, Dean KES, Kirby AJ (1999) A mechanism for efficient proton-transfer catalysis: intramolecular general acid catalysis of the hydrolysis of 1-arylethyl ethers of salicylic acid. Can J Chem 77:792–801
44. Asaad N, Davies JE, Hodgson DRW, Kirby AJ (2005) The search for efficient intramolecular proton transfer from carbon: the kinetically silent intramolecular general base-catalysed elimination reaction of o-phenyl 8-dimethylamino-1-naphthaldoximes. J Phys Org Chem 18:101–109
45. Kirby AJ, Parkinson A (1994) Most efficient intramolecular general acid catalysis of acetal hydrolysis by the carboxyl group. J Chem Soc Chem Commun 707–708
46. Kirby AJ, Lima MF, de Silva D, Roussev CD, Nome F (2006) Efficient intramolecular general acid catalysis of nucleophilic attack on a phosphodiester. J Am Chem Soc 128:16944–16952
47. Hartwell E, Hodgson DRW, Kirby AJ (2000) Exploring the limits of efficiency of proton-transfer catalysis in models and enzymes. J Am Chem Soc 122:9326–9327
48. Kirby AJ, Williams NH (1994) Efficient intramolecular general acid catalysis of enol ether hydrolysis: hydrogen-bonding stabilization of the transition state for proton transfer to carbon. J Chem Soc Perkin Trans 2:643–648
49. Kirby AJ, Williams NH (1991) Efficient intramolecular general acid catalysis of vinyl ether hydrolysis by the neighbouring carboxylic acid group. J Chem Soc Chem Commun 1643–1644
50. http://w/w/w.gaussian.com
51. Casewit CJ, Colwell KS, Rappé AK (1992) Application of a universal force field to main group compounds. J Am Chem Soc 114:10046–10053
52. Dewar MJS, Zoebisch EG, Healy EF, Stewart JJP (1985) AM1: a new general purpose quantum mechanical molecular model. J Am Chem Soc 107:3902–3909
53. Murrell JN, Laidler KJ (1968) Symmetries of activated complexes. Trans Farad Soc 64:371–377
54. Muller K (1980) Reaction paths on multidimensional energy hypersurfaces. Angew Chem Int Ed Eng 19:1–13
55. Perrin DD, Dempsey B, Serjeant EP (1981) pKa prediction for organic acids and bases. Champan & Hall, London
56. The percentage of the ionized and unionized forms was calculated using Henderson-Hasselbach equation
57. Kirby AJ (1980) Effective molarities for intramolecular reactions. Adv Phys Org Chem 17:183 and references therein